The mineralogy and origin of hydrothermally altered Quaternary volcanic rocks on the south flank of Lassen volcano, California: Interim report for USGS Mineral Resource External Research Program grant of $42,000 in FY 2005

November, 2005

Robert G. Lee[1], John H. Dilles[1], David A. John[2], Tanya L. Abela[1]

[1]Department of Geosciences Oregon State University, Corvallis, OR 97331-5506
[2]U.S. Geological Survey, MS-901, 345 Middlefield Rd., Menlo Park, CA 94025

rglee@geo.oregonstate.edu

Abstract

Lassen Volcanic National Park hosts the largest active hydrothermal system in the Cascade Range in association with recent dacitic volcanism centered on Lassen Peak, one of the most active of the Cascade volcanoes. The modern hydrothermal system affects rocks in a >0.5 km2 area and is principally expressed as an east-west trending zone extending 3 km along the south flank of the volcano from the hot springs at Bumpass Hell westward across Little Hot Springs Valley to Sulphur Works. Older and inactive hydrothermal alteration systems affected rocks in a >2 km2 area that extends west to Brokeoff Mountain, as well as north and southwest. These zones are exposed in nearly 500 m of relief in the eroded core of the Pleistocene Brokeoff volcano. Geologic mapping has identified a series of andesite dikes and plugs within the Brokeoff volcano, which suggest that Brokeoff constituted a volcanic field rather than a single stratovolcano. Several intrusive centers are located within and apparently are related to several ancient hydrothermal alteration zones, which vary in character from one center to another.

During field mapping more than 200 rock samples were collected in a two km^2 area extending from Bumpass Hell to Sulphur Works and analyzed with a field-portable, short-wave inferred spectrometer to identify hydrous silicate alteration minerals. A subset of these samples were characterized in the laboratory in more detail via X-ray diffraction (47 bulk rock and <15 um fractions), petrography, scanning electron microscopy (10), and whole-rock geochemistry (24). From these mineralogic identifications a series of mineral distribution maps were plotted and synthesized in an alteration assemblage map.

The active hydrothermal system consists of steam-heated alteration produced where ascending H_2S-rich steam condenses at the water table near the surface. The active hot springs and fumaroles have temperatures of up to 160°C at Bumpass Hell, but more typically <80°C. The main east-west trend of hot springs from Sulphur Works to Bumpass Hell and beyond the field area to Devils Kitchen is locally controlled by east-west striking faults. A subsidiary set of hot springs are aligned north-south in Little Hot Springs Valley and at Sulphur Works, and principally occur in Holocene post-glacial landslide and colluvial deposits Steam-heated active system produces low temperature alteration of rock to mixtures of kaolinite, alunite, opal, and cristobalite with accessory iron sulfates near surface and pyrite below the water table.

The older and inactive hydrothermal systems produced a series of alteration zones dominated by intermediate argillic and propylitic alteration in Little Hot Springs Valley and near Sulfur Works. In the basaltic andesite lavas in the bottom of Little Hot Springs Valley, waters produced illite/smectite, chlorite, calcite, quartz, pyrite, albite, and K-feldspar whereas at higher elevations silicic andesites are altered to montmorillonite or illite-smectite with minor pyrite. On the southeast flank of Pilot Pinnacle a separate hydrothermal center contains a zone of intermediate argillic alteration cored by advanced argillic alteration characterized by mixtures of pyrophyllite, dickite, alunite, kaolinite, and quartz. The presence of quartz, calcite, and pyrite-bearing veins within the intermediate argillic alteration suggests that the inactive alteration zones were produced by condensed hydrothermal waters when the water table was higher than at present. Hydrogen isotopic analyses of altered rocks in both the active and inactive alteration

zones yield a range of ∂D from -100 to -130 permil, consistent with origins from hydrothermal fluids dominated by local meteoric water.

Introduction

Active and fossil hydrothermal systems are present in many of the Quaternary Cascades volcanoes, but the distribution, composition, and origin of hydrothermal alteration products is generally poorly known for the Cascades. These hydrothermal systems are the result of shallow subvolcanic magmatic-hydrothermal environments and are of interest because of the world-wide association with epithermal gold-silver deposits (Arribas, 1995; Hedenquist et al., 2000) that may root into base-metal deposits (Sillitoe and Hedenquist, 2003). Hydrothermal alteration can also weaken volcanic edifices and cause slope instability and structural collapse (Siebert, 2002). By studying the hydrothermal alteration it may be possible to determine what controls the distribution and mineralogy of alteration as well as how structure and lithology may control alteration.

The south flank of Lassen Peak, northern California hosts the largest active magmatic-hydrothermal system in the Cascade Range. Here, both active and fossil hydrothermal systems are exposed in eroded Pleistocene rocks of Brokeoff volcano. The active systems extends approximately 12 km from the western boiling mud pots and fumaroles at Sulphur Works, eastward across Little Hot Springs Valley (LHSV), to the largest thermal pools at Bumpass Hell on the east, and eastward beyond the study area to Terminal Geyser (Figure 1). The hydrothermal systems are characterized by steam-heated alteration (Ingebritsen and Sorey, 1987) that is locally superimposed on alteration

zones produced by older and inactive higher temperature and water-dominated hydrothermal systems (Crowley et al., 2004).

The active Lassen hydrothermal system is characterized by a two-phase system with a vapor-dominated reservoir centralized beneath the Bumpass Hell area lying above a liquid-dominated system. Steam rises to discharge at the higher elevations as fumaroles and acid-sulfate springs, whereas alkali-chloride liquid discharges laterally to the south at Morgan and Growler hot springs and south-southeast at Terminal Geyser. Ingebritsen and Sorey (1987) modeled the Lassen hydrothermal system as a liquid-dominated zone below Bumpass Hell with a parasitic vapor-dominated zone above the boiling liquid. Xu and Lowell (1998) suggested that the hydrothermal system is not static but oscillatory on a period of ~1000 years. This system controls the formation of steam-heated acid alteration in the active areas of hydrothermal alteration.

The alteration that resulted from the older and inactive hydrothermal systems is well exposed in a zone extending from Brokeoff Mountain eat to Bumpass Hell and to the northeast to Pilot Pinnacle. Remote sensing spectral analysis has identified illite-smectite alteration in these zones (Crowley et al., 2004), parts of which are characterized with moderate oxygen isotopic depletion as documented by Rose et al. (1994).

This report is based on research by Oregon State University (OSU) in collaboration with the Mineral Resource Program of U.S. Geological Survey (USGS-MRP). The Oregon State University research was supported by the Mineral Resource External Research Program (MSERP) grant for the federal fiscal year 2005.

The objective of the research program reported below was to document the distribution and composition of hydrothermal alteration mineral products on the south

flank of Lassen Volcano in order to understand the origin of the alteration, the mineral resource potential, and slope failure mechanisms and hazards.

Regional Geology

The Lassen volcanic region is located at the southern extent of the Cascades volcanic arc in northern California (Figure 1a). Volcanism is related to the northwestward subduction of the Gorda plate, part of the Juan de Fuca plate system (Guffanti and Weaver, 1988). The Lassen region lies along the western margin of the Basin and Range extensional province that lies east of the Cascades (Pezzopane and Weldon, 1993). This extensional system transects the Lassen area and is characterized by normal and right-oblique slip normal faults (Figure 1b) and volcanic vents that are aligned in a north-northwest direction (Guffanti et al., 1990; Guffanti et al., 1996). Volcanism has occurred in the Lassen region for approximately the last 7 million years and can be characterized on two scales (Clynne, 1990). On a regional scale hundreds of small, short-lived, mafic to intermediate composition volcanoes occur throughout the Lassen region. Superimposed over this are a few larger, longer-lived, basaltic to rhyolitic volcanic centers. The Caribou volcanic field (CVF Figure 1b) consists of approximately 50 km^3 of erupted material from over 100 small cones and shields at 700 to 20 ka (Clynne and Muffler, 1990; Guffanti et al., 1996). These cones are constructed of olivine-pyroxene basaltic andesites and andesites, olivine basalt, and pyroxene andesites (Guffanti et al., 1996). The Lassen volcanic center (LVC Figure 1b) is the youngest of five volcanic centers including Latour, Dittmar, Yana, and Maidu. These volcanic centers generally evolved from an initial cone-building episode of basaltic to andesite lava flows and a late-stage emplacement of dacite to rhyolite domes and flows on the

flanks of the main composite cone (Clynne, 1984; 1990). The LVC began with the construction of Brokeoff volcano, which was an andesitic stratocone active from 600 to 400 ka (Clynne, 1990). The Brokeoff volcano is overlain by three successively erupted sequences of dacitic to rhyolitic lava flows: the Rockland sequence at ~400 ka; the Bumpass sequence from 250 to 200 ka; and the Loomis sequence 100 ka to present (Clynne, 1990). Lassen Peak is a dacitic dome complex that represents the youngest stage of silicic eruptions in the LVC. Lassen Peak formed at 26 to 28 ka (Turrin et al., 1998), and the most recent eruptions occurred in 1914 and 1915 (Clynne, 1999).

Fossil hydrothermal systems and hydrothermal alteration mineralogy have been described in the Lassen region at Maidu (Wilson, 1961; John et al., 2005) and at Brokeoff volcano (Rose et al., 1994; Crowley et al., 2004). Maidu hosts a fossil acid-sulfate magmatic-hydrothermal system in the eroded core of the late Pliocene volcanic center. Both active and fossil systems are found at Brokeoff volcano (Figure 1C), with fossil systems concentrated in the eroded center of the stratocone extending from Brokeoff Mountain to LHSV. Active hydrothermal systems occur within the stratocone and extend laterally to the south and southeast.

Geology of Brokeoff Volcano

Brokeoff volcano is located in the southeast corner of the Lassen Volcanic Center, and has been described as an eroded andesitic stratocone (Williams, 1932: Figure 1C). The general stratigraphy of the volcano consists of two stages of magmatism. The first stage is the Mill Creek sequence erupted between 600 and 475 ka and consists multiple flows of glassy basaltic andesites and two-pyroxene andesites, along with pyroclastic and

other fragmented deposits with variable (5 to 40%) phenocrysts (Clynne 1990). The second stage, the Diller sequence, erupted from 475 to 400 ka and consists of thick andesite flows with 30-40% phenocrysts of plagioclase, hypersthene, augite, and titanomagnetite. Aproximately 500 m of the first stage is exposed in the glacial and fluvial valleys and ridges between Brokeoff Mountain and Sulphur Works and in Little Hot Spring Valley, whereas the second stage occurs at higher elevations mainly to the north and west of these locations (Figure 2). To the northeast above Bumpass Hell are a series of two-pyroxene-hornblende dacite domes that make up the Bumpass sequence. Based on the dips of the lava flows the central part of the volcano is believed to occur at Diamond Peak (Clynne, 1990), which is composed of intrusive bodies, lava flows, and brecciated flows. Brokeoff Mountain, Mount Diller, Pilot Pinnacle, and Mount Conard are believed to represent the flanks of the main volcano (Clynne, 1990; Clynne et al., 2002). Maximum elevation of the original cone is believed to have been 3400 m (Williams, 1932) and the basal diameter is estimated to be about 12 km with roughly 80 km^3 volume (Clynne, 1990).

The volcano has been deeply eroded by glacial and fluvial processes creating an irregular, bowl shaped depression south of Lassen Peak and the deeply incised Mill Creek canyon. LHSV located in the northern part of Mill Creek canyon cuts into the center of Brokeoff volcano exposing an older intermediate argillic alteration. Numerous landslide and glacial deposits occur in valleys and side drainages where active fumaroles and acid-sulfate springs are concentrated. We suggest that these weak porous materials are either conduits for the uprising steam, or that the resulting sulfataric decomposition of the lavas is promoting slope instability in these areas. Locally intense and widespread sulfataric

hydrothermal alteration occurs throughout a 6 to 7 km bowl that makes up the center of Brokeoff volcano with the largest areas located at Bumpass Hell and Sulphur Works. These active areas of hydrothermal alteration are the result of a vapor-dominated acid-sulfate system (Muffler et al., 1982; Ingebritsen and Sorey, 1985). Additionally, Little Hot Springs Valley hosts an older liquid-dominated system (Crowley et al., 2004) and Brokeoff Mountain host an older acid-sulfate alteration currently being investigated in detail by D. John and co-workers.

During mapping of the area several plugs and radiating andesite dikes have been found throughout the area (Figure 2). Petrographically these dikes are similar to the two-pyroxene andesites of the Mill Creek sequence and Mount Diller sequence suggesting these dikes may be the feeders for these lavas. We suggest that Brokeoff Volcano was a volcanic field with several vents and domes rather than a stratovolcano as initially described.

Methodology

During the summers of 2004 and 2005 approximately five weeks were spent on the southern flank of Lassen Volcano. Geologic and hydrothermal alteration minerals were mapped on topographic and DOQ base maps. A total of 269 samples were collected for laboratory analysis and located to (±5 m) with a GPS unit. A Portable Infrared Mineral Analyzer (PIMA™) was used in the field for rapid identification of hydrous alteration minerals (excepting Fe-hydroxieds and oxides) in excess of 5 to 10 vol. % of sample. Short-wave infrared (SWIR) spectrometers can identify hydrous minerals at the 5 to 10 volume percent level in order to characterize high-sulfidation and low-sulfidation epithermal environments (Thompson et al., 1999). The spectra were analyzed in order to

identify minerals present using characteristic absorption features of wavelength position, depth, and width (Figure 3), which are a function of molecular bonds present in the mineral (Thompson et al., 1999). The computer database software FEATURESEARCH™ and SPECMIN™ were used to identify absorption features by comparison with mineral reference libraries. Figure 4 shows some representative spectra of samples analyzed in the field.

X-ray powder diffraction patterns were analyzed on forty-seven samples using a Phillips XRG 446, run at 40 kilovolts and 30 milliamps using a copper Kα radiation source. Samples were chosen for a detailed analysis of clay mineralogy and to confirm initial PIMA identification. Analyses were performed on bulk rock powders, <15 μm size fractions, and <2 μm size fractions. The mineralogy of samples was identified using the characteristic mineral d-spacing of X-ray emission lines according to procedures detailed in Moore and Reynolds (1997) and using the Jade™ 3.0 software.

Ten samples were analyzed on an Amray 3300 field emission scanning electron microscope (FESEM) housed at the Oregon State University electron microscope facility. Samples were broken into small chips approximately 2-3 cm in diameter and glued to stands. The samples were then coated with a 60% Au 40% Pd mixture and vacuum sealed in the machine. An X-ray energy dispersive spectrometer was used to identify semi-quantitatively the major element concentrations within image.

Sixteen whole rock and <15 μm samples were analyzed for D/H isotopic composition using a TC/EA furnace operating at 1450ºC on line with a gas chromatograph and continuous flow mass spectrometer at Oregon State University. Whole rock and <15 μm samples were weighed out to approximately 2 mg and placed in

silver capsules. The samples were heat treated in a vacuum oven at 50-70 ºC for approximately 2 hours to evaporate excess water. Samples were standardized using an in house National Bureau of Standard biotite (NBS-30, -65 ‰) and reported in permil notation relative to VSMOW. Analytical reproducibility on unknowns is ± 2 permil (n = 5).

Hydrothermal alteration mineralogy

Figure 5 shows the sample locations and distribution of major alteration minerals in the Brokeoff Volcano area.

Intensely and pervasively altered rocks are located in the valleys and bowls near Sulphur Works, Pilot Pinnacle, LHSV, and Bumpass Hell (Figure 6). Active fumaroles and mud pots within Sulphur Works and Bumpass Hell have formed advanced-argillic steam-heated alteration forming the largest active hydrothermal system in the Cascades. Sulphur Works lies within andesites of the Mill Creek Sequence and Quaternary landslide material. Bumpass Hell is confined to a bowl-like depression within dacite lavas and vent breccias from the Bumpass Sequence as well as Quaternary colluvial deposits. The lower slopes of Pilot Pinnacle have active fumaroles within landslide deposits whereas the higher slopes host higher temperature argillic alteration. LHSV hosts an inactive water-dominated near-neutral alteration that extends from the Mill Creek stream channel to midway up the slopes and cliffs to the east and west (Crowley et al., 2004). This older system is concentrated within flow breccias of the Mill Creek sequence and extends upwards into flow breccias and andesites of the Mount Diller sequence. Active hot

springs are confined to the stream bed of Mill Creek in the center section of LHSV, and on the south east slopes of the valley.

Bumpass Hell

Bumpass Hell consists of superheated steam vents and acid-sulfate hot springs (Janik et al., 1983) that are related to active steam-heated acid-sulfate alteration. The acidic alteration covers approximately 1 km from east to west and approximately 0.5 km from north to south in Bumpass Hell, yet active steam venting extends approximately 200m on an NW-SE trend in the central part of the area (Figure 5). Surrounding the steam-heated alteration is a region of weakly acidic to near-neutral smectite-rich alteration (Figure 5). Major alteration minerals within Bumpass Hell characteristic of the acid-sulfate alteration include kaolinite, alunite, cristobalite, and opal (Figure 4, 6a). Alteration is pervasive, and most of the original rock host has been completely altered with few relict textures remaining. Kaolinite is present in most of the samples in Bumpass Hell and occurs in great abundance within the western edge of the area (Figure 6a). Kaolinite is typically fine grained (≤20 μm) and commonly associated with opal or montmorillonite. Alunite occurs within the altered slopes to the north and west of the central Bumpass Hell area and is commonly associated with kaolinite, ferric and ferrous hydroxides and sulfate minerals, and cristobalite (Figure 7e, f). Alunite typically forms fine-grained (≤10 μm) tabular crystals with a sugary texture in hand specimen. SEM images show alunite as platy to tabular, mica-like crystals ≤5 μm long filling vugs and growing on and around kaolinite grains (Figure 8a, b). PIMA and XRD analyses indicate that alunite compositions range from K-rich alunite to Na-rich alunite throughout the Brokeoff volcano region. At Bumpass Hell the composition of alunite is K-rich whereas

Na-bearing alunites occur in samples located farther away from the more active steam-heated regions. Alunite appears to be the dominant mineral in the slopes surrounding Bumpass Hell whereas kaolinite and opal mixtures are dominant in the central zone of hot spring venting (Figure 6a, Figure 9c). Silica phases are extensive within the area and include quartz, cristobalite, and opal. Opaline silica is the most abundant phase in the central part of the region where the greatest steam activity occurs. Microcrystalline quartz, cristobalite, and calcedonic silica are found in the northern and southern slopes above Bumpass Hell. Quartz and chalcedony possibly formed in a near-neutral liquid-dominated alteration predating the active system. Other minerals present include anatase, hematite, goethite, jarosite, native sulfur, and unknown sulfate minerals. Goethite, hematite, and jarosite were all observed petrographically and in XRD analysis (Figure 7e), with goethite staining occurring as wide (1-2 m) bands surrounding the active center of Bumpass Hell but distinctly lacking in the central area near the thermal pools. Native sulfur and sulfate minerals occur near the active steam regions. Montmorillonite is generally abundant in the slopes surrounding Bumpass Hell, but also occurs in the center of the system with kaolinite and opal (Figure 5b).

Little Hot Springs Valley

LHSV contains two areas of alteration with the Upper section located in a small area (1/3 km^2) the northern section of the valley and the Lower section encompassing all the alteration to the south and east in LHSV (Figure 6). Upper LHSV encompasses an area that has a both active and fossil travertine deposits first noted by Muffler and Clynne, (in press, personal communication, 2005). To the west of these carbonate springs are steam-heated advanced argillic alteration that extends west up to Highway 89.

South of the travertine deposits are deposits of intermediate argillic alteration (Figure 6). An outcrop of andesite breccia from the Mill Creek sequence within the Upper LHSV alteration contains pyrophyllite (Figure 4), and is surrounded by smectite.

Alteration in the Lower LHSV encompasses approximately two square kilometers and extends from Mill Creek up to the ridges of LHSV. Active steam vents and boiling mud puts occur in the central part of the valley and on the southern slope of a small side valley extending from Mill Creek east to the ridge line (Figure 9a). Major minerals associated with alteration in this small valley include kaolinite, alunite, and opal. PIMA analyses indicate that much of the kaolinite is associated with smectite. Figure 6 shows the distribution of kaolinite and smectite in the valley and Crowley et al. (2004) noted this mixture and suggested that steam-heated alteration is overprinting an older alteration assemblage. The steam-heated alteration is confined in landslide and slump deposits (Figure 9a). In the center of the steam-heated alteration is a series of at least five travertine pools. One of the pools sampled in the summer of 2005 had a temperature of 87.5ºC and a pH of 6.25 (Muffler, personal communication, 2005). Fumaroles and steam vents are located both 10 to 20 m to the north and west of the travertine deposits. Within the central LHSV advanced argillic alteration of steam-heated origin is confined to the active steam vents and does not extend more than one to two meters into the intermediate argillic alteration.

The major mineralogy in the main LHSV includes montmorillonite, pyrite, feldspar, illite/smectite, chlorite, calcite, and silica. Adularia has been found in this assemblage in trace amounts but is rare. We suggest that this alteration assemblage is an intermediate argillic alteration that formed when the water table was higher than it is

currently. The intermediate argillic alteration occurs in flow breccias that are capped by weakly smectite altered andesite lava flows. Original rock textures are typically preserved, but in some cases complete replacement of phenocrysts and groundmass has occurred. Montmorillonite replaces the groundmass and partially replaces plagioclase and mafic mineral phenocrysts, and is associated with pyrite and microcrystalline quartz. Up to 5% pyrite occurs in some areas as fine, to very-fine disseminated grains within the groundmass (Figure 8c). Pyrite is typically fine-grained (≤50-60 μm diameter), but some grains have been found in excess of 3-4 mm. Grains are typically euhedral and may form narrow veins within the alteration. Pyrite is the only sulfide mineral identified in the area. Albite is the common feldspar mineral in the alteration assemblage but orthoclase has been found in XRD and SEM analyses (Fig 7c, 8e). Orthoclase forms small tabular crystals commonly found with platy montmorillonite growing around it. Illite replaces the groundmass and is typically associated with montmorillonite and pyrite (Figure 8c, d). Chlorite is associated with montmorillonite as a replacement of primary igneous mafic minerals in the groundmass (Figure 7c, 8h). Both illite and chlorite are fine grained (≤20 μm) and are generally disseminated. Calcite is coarse- to fine-grained, generally filling vugs and porous spaces in lava flows and disseminated throughout the groundmass in the brecciated layers (Figure 8g). At lower elevations in along the stream channels in LHSV small narrow (2-4 mm) veins of calcite have been observed. At higher elevations (~7700 ft), the intermediate argillic alteration is a mineralogically distinct due to the lack of chlorite and calcite (Figure 9b). The main silica phase is microcrystalline quartz typically associated with pyrite.

Pilot Pinnacle

Areas of hydrothermally altered rock in the Pilot Pinnacle area extend from the ridge below Pilot Pinnacle southeast down to the State Highway 89 (Figure 6). Active steam vents and boiling mud pots occur in glacial and colluvial deposits at the base of Pilot Pinnacle and are associated with steam-heated advanced argillic alteration similar to Bumpass Hell and LHSV. In the upper slopes and along the roadside, the alteration mineralogy includes pyrophyllite, dickite, and natroalunite with accessory quartz, illite, and Fe-oxide minerals. Pyrophyllite is present in one sample on the slope below Pilot Pinnacle where it is associated with natroalunite, kaolinite, and jarosite (Figure 4, 7b, 8F). Pyrophyllite is fine-grained (≤10 μm) and forms platy grains on the edges of cavities and vugs. Dickite occurs in the lower areas of Pilot Pinnacle and forms a large outcrop (3-4 m high) along the road. The outcrop is completely altered with no relict textures or minerals. The dickite is fine-grained (≤10 μm) and is associated with illite, anatase (Figure 7a), alunite, and quartz. This alteration assemblage may be an older inactive advanced argillic alteration.

Sulphur Works

We have split Sulphur Works into two areas of alteration, upper Sulphur Works and lower Sulphur Works (Figure 6). Steam-heated advanced argillic alteration is associated with active fumaroles and boiling springs in both upper and lower Sulphur Works along a north-south trend. Located at the base of altered zone at the south side of lower Sulphur Works in the main discharge stream are two large (3-4 m diameter) travertine deposits associated with hot springs having a temperature at 84ºC (Muffler, personal communication, 2005). Acid-sulfate alteration assemblages are similar to those of lower LHSV and Bumpass Hell: kaolinite, alunite, opal, anatase, and/or rutile minerals

(Figure 7d) are associated with the steam-heated zones, whereas montmorillonite, illite, and pyrite characterize the intermediate argillic alteration (Figure 6). Steam-heated alteration is typically pervasive with little to no relict textures remaining in the host material.

Hydrothermal alteration structures

Structural features include altered dikes and plugs, faults, quartz/chalcedony veins, calcite veins, and hydrothermal breccias. These are broadly distributed throughout the area of study. To the west of Sulphur Works are a series of elongate silicified zones composed of microcrystalline to fine-grained quartz, alunite, and Fe-oxide minerals. These features have not been observed in the LHSV or Bumpass Hell areas. The distinctive silica ledges most likely represent locations of upward fluid flow of low pH condensed fluid.

Geochemistry

A total of 74 samples were submitted to the USGS at Menlo Park for geochemical analysis (Table 3). These rocks were sampled based on alteration mineralogy, texture, structure and several unaltered samples were also submitted for control of elemental distribution during alteration.

Acid water and steam from active thermal springs in the Brokeoff volcano area have low pH and high sulfate concentrations (Muffler et al., 1982; Janik et al., 1983; Thompson, 1985) and define a kinetic isotope fractionation trend on a δD versus $\delta^{18}O$

diagram (Figure 10). Deuterium values for active and inactive hydrothermally altered minerals range from -130 to -100 per mil (Table 2).

Discussion

Hydrothermal and major mineralogical features of Brokeoff volcano area can be defined by three alteration assemblage types: 1) advanced argillic with pyrophyllite and dickite; 2) steam-heated advanced argillic with kaolinite, alunite, cristobalite, and opal; and 3) intermediate argillic with montmorillonite, pyrite, and illite/smecite (Table 1). Figure 10 shows the alteration assemblage map we have determined from the results of our mapping and analysis.

Advanced argillic alteration around Pilot Pinnacle and upper LHSV suggests higher temperature acid-sulfate fluid may have been centered in this area. The presence of pyrophyllite-alunite suggests temperatures ≥ 230ºC with pH ≤ 2, however the presence of dickite, quartz, and illite suggests temperatures between 200 and 300ºC (Reyes, 1990; Arribas, 1995; Hedenquist et al., 2000). Both kaolinite and montmorillonite occur around the advanced argillic alteration similar to characteristics of high-sulfidation epithermal deposits (Arribas, 1995).

Intermediate argillic alteration in the center of the Brokeoff edifice suggests moderate elevated temperatures within a liquid-dominated reservoir, characterized by neutral pH conditions (Muffler et al, 1982). Crowley et al. (2004) suggested two different alterations within the presence of mixed layer illite/smectite clays with propylitically-altered chlorite alteration. We have found altered areas with both chlorite and illite mixtures, but illite/smectite alteration is dominant in the permeable flow top

breccias. Chlorite appears to be stratigraphically controlled with calcite in lower elevations of the Brokeoff edifice. The lack of chlorite/calcite in intermediate argillic alteration above 7700 feet in LHSV suggests this may be a transition zone with the location of the water table during active alteration.

The acid-sulfate steam heated alteration formed from a shallow vapor-dominated reservoir beneath areas of active solfataric systems (Ingebritsen and Sorey, 1987). Kaolinite and alunite mixtures are products of this alteration environment with montmorillonite most likely a feature of the intermediate argillic alteration. The presence of kaolinite and montmorillonite mixtures in LHSV and in areas of Bumpass Hell likely represent an overprinting of the two hydrothermal environments (Crowley et al., 2004). This overprinting is most likely due to a drop in the water table as the kaolinite-alunite alteration in the LHSV is currently active. The change in the propylitic chlorite alteration at roughly the same elevation to the north of the kaolinite-montmorillonite mixtures in LHSV is further evidence for a change in the water table.

Summary

Over two hundred and fifty samples were collected from Lassen Volcanic National Park and were analyzed using a variety of methods. Alteration products were mapped and define three distinct alteration assemblages in the park. Inactive fossil alteration assemblages are the result of two different hydrothermal systems of acid-sulfate and near-neutral argillic alteration. Active vapor-dominated advanced argillic alteration defines the current alteration at the surface of the Brokeoff volcano region.

Future work for this project includes the analysis of the geochemistry from samples submitted to the USGS, fluid inclusion work on quartz mineral separates collected from the Lassen area, and deuterium and oxygen work on clay separates from the samples collected in the park. Plans to publish the findings from this study are set for next year when all analyses have been completed.

References

Arribas, A., Jr., 1995, Characteristics of high-sulfidation epithermal deposits, and their relation to magmatic fluid: *In* Magmas, fluids, and ore deposits, Thomspon, J.F.H., ed., Mineral Association of Canada Short Course Series, v. 23, p. 419-454.

Bullen, T.D., and Clynne, M.A., 1990, Trace element and isotopic constraints on magmatic evolution at Lassen Volcanic Center: Journal of Geophysical Research, v. 95, p. 19,671-19,691.

Clynne, M.A., 1990, Stratigraphic, Lithologic, and major element geochemical constraints on magmatic evolution at Lassen Volcanic Center, California: Journal of Geophysical Research, v. 95, p. 19,651-19,669.

Clynne, M.A., Janik, C.J., and Muffler, L.J.P., 2002, "Hot Water" in Lassen Volcanic National Park – Fumeroles, Steaming Ground, and Boiling Mudpots: U.S. Geological Survey Fact Sheet 101-02.

Crowley, J.K., Mars, J.C., John, D.A., Muffler, L.J.P., and Clynne, M.A., 2004, Hydrothermal mineral zoning within an eroded stratocone: Remote sensing spectral analysis of Brokeoff volcano, California, *in* King, P.L., Ramsey, M.S., and Swayze, G.A., eds., Infrared Spectroscopy in Geochemistry, Exploration Geochemistry, and Remote Sensing, Minerological Association of Canada Short Course, v. 33, p. 215-226.

Guffanti, M., and Weaver, C.S., 1988, Distribution of late Cenozoic volcanic vents in the Cascade Range: Volcanic arc segmentation and regional tectonic considerations: Journal of Geophysical Research, v. 93, p. 6513-6529.

Guffanti, M., Clynne, M.A., Smithm J.G., Muffler, L.J.P., and Bullen, T.D., 1990, Late Cenozoic volcanism, subduction, and extension in the Lassen region of California, southern Cascade Range: Journal of Geophysical Research, v. 95, p. 19,453-19,464.

Guffanti, M., Clynne, M.A., and Muffler, L.J.P., 1996, Thermal and mass implications of magmatic evolution in the Lassen volcanic region, California, and minimum constraints on basalt influx to the lower crust: Journal of Geophysical Research, v. 101, p. 3003-3013.

Hedenquist, J.W., and Lowenstern, J.B., 1994, The role of magmas in the formation of hydrothermal ore deposits: Nature, v. 370, p. 519-527.

Hedenquist, J.W., Arribas, A., Jr., and Gonzalez-Urien, E., 2000, Exploration for epithermal gold deposits, *in* Hagemann, S.G., and Brown, P.E., eds., Gold in 2000: Rev in Econ. Geology, v. 13, p. 245-277.

Henley, R.W., and Ellis, A.J., 1983, Geothermal Systems ancient and modern: a geochemical review: Earth-science reviews, v. 19, p. 1-50.

Ingebritsen, S.E., and Sorey, M.L., 1985, A quantitative analysis of the Lassen hydrothermal system, North Central California: Water Resources Research, v. 21, p. 853-868.

Ingebritsen, S.E., and Sorey, M.L., 1987, Conceptual models for the Lassen hydrothermal system: Geothermal Resources Council Bulletin, v. 16, p. 3-9.

Ingebritsen, S.E., Mariner, R.H., and Sherrod, D.R., 1994, Hydrothermal systems of the Cascade Rance, North-Central Oregon: U.S. Geological Survey Professional Paper 1044-L, 86p.

Janik, C.J., Nehring, N.L., and Truesdell, A.H., 1983, Stable isotope geochemistry of thermal fluids from Lassen Volcanic National Park, California: Geothermal Resources Council, Transactions, v. 7, p. 295-299.

Muffler, L.J.P., Nehring, N.L., Truesdell, A.H., Janik, C.J., Clynne, M.A., and Thompson, J.M., 1982, The lassen Geothermal System: Pacific Geothermal Conference 1982, Auckland, New Zealand, p. 349-356.

Moore, D.M., and Reynolds, R.C., Jr., 1997, X-ray diffraction and the identification and analysis of clay minerals: Oxford University Press, N.Y., 378 p.

Pezzopane, S.K., and Weldon R.J. II., 1993, Tectonic role of active faulting in central Oregon: Tectonics, v. 12, p. 1140-1169.

Reyes, A.G., 1990, Petrology of Philippine geothermal systems and the application of alteration mineralogy to their assessment: Journal of Volcanology and Geothermal Research, v. 43, p. 279-309.

Rose, T.P., Criss, R.E., and Mughannam, A.J., 1994, Oxygen isotope evidence for hydrothermal alteration within a Quaternary stratovolcano, Lassen Volcanic National Park, California: Journal of Geophysical Research, v. 99, p. 21,621-21,633.

Sillitoe, R.H., 1993, Epithermal models: genetic types, geometrical controls and shallow features, *in* Kirkham, R.V., Sinclair, W.D., Thorpe, R.I., and Duke, J.M., eds., Mineral Deposit Modeling, Geological Association of Canada Special Paper 40, p. 403-418.

Thompson, A.J.B., Hauff, P.L., and Robitaille, A.J., 1999, Alteration mapping in exploration: application of Short-Wave Infrared (SWIR) spectroscopy: Soc. Econ. Geol. Newsl 39, 13p.

Thompson, J.M., 1985, Chemistry of thermal and nonthermal springs in the vicinity of Lassen Volcanic National Park: Journal of Volcanology and Geothermal Research, v. 25, p. 81-104.

Turrin, B.D., Christiansen, R.L., Clynne, M.A., Champion, D.E., Gerstel, W.J., Muffler, L.J.P., and Trimble, D.A., 1998, Age of Lassen peak, California, and implications for the ages of late Pleistocene glaciations in the southern Cascade Range: GSA Bulletin, v. 110, p. 931-945.

Williams, H., 1932, Geology of the Lassen Volcanic National Park, California: University of California Publications, Bulletin of the Department of Geological Sciences, v. 21, 195-385.

Wilson, T.A., 1961, The geology near Mineral, California: Berkeley, University of California, M.S. thesis, 92 p.

White, D.E., Muffler, L.J.P., and Truesdell, A.H., 1971, Vapor-Dominated Hydrothermal Systems compared with hot-water systems: Economic Geology, v. 66, p. 75-97.

Xu, W., and Lowell, R.P., 1998, An alternative model of the Lassen hydrothermal system, Lassen Volcanic National Park, California: Journal of Geophysical Research, v.103, p. 20,869 - 20,881.

Figure Captions

Figure 1. A: Tectonic setting of the Cascade Arc with rectangular insert denoting location of Lassen volcanic region. B: Map of the the Lassen volcanic region showing the major normal vaulting in the area. Irregular lines outline the vent fields of Lassen volcanic center (LVC) and Caribou volcanic field (CVF). Stars denote the locations of the other major volcanic centers: L, Latour; Y, Yana; D, Dittmar; and M, Maidu. Brokeoff volcano (BV) is dashed circle. Figure modified from Ingebritsen and Sorey (1985) and Guffanti et al. (1996). C: South east section of the Lassen region showing active hydrothermal systems in red and fossilized systems in green. Modified from Clynne et al. (2002). Solid rectangle marks location of figure 2.

Figure 2. Geologic map of the Brokeoff Volcano region showing rock sequences, structure, active fumaroles and intrusive dikes and plugs. Geology from Clynne and Muffler (in press) and this study.

Figure 3. A: Infrared spectra of dickite and kaolinite (samples CALV053 and CALV262) showing the distinguishing characteristics for identification including the hull, feature depths, position, and the full width half-maximum. Dickite has doublet feature depths at 1.384 and 1.414, while kaolinite has doublet feature depths at 1.396 and 1.414. Kaolinite also has a higher full width half-maximum (inset). B: Spectra patterns of sample CALV262 vs. USGS Denver kaolinite standard. C: Spectra patterns of sample CALV053 vs. USGS Denver dickite standard. Large absorbance at 1.9 in CALV053 is from excess water in the sample as apposed to the standard.

Figure 4. Infrared spectroscopy images from Bumpass Hell, Pilot Pinnacle, Upper Little Hot Springs Valley (LHSV), and Lower Little Hot Springs Valley (LHSV). Numbers to right of pattern indicate sample name and bold face mineral name/mixture above pattern indicates sample type.

Figure 5. Sample maps denoting major mineral locations for the Brokeoff volcano area. Geology contacts same as in Figure 2.

Figure 6. Map of the hydrothermal alteration assemblages in the Brokeoff Volcano region. Geologic contacts are same as in figure 2.

Figure 7. XRD spectral patterns for Brokeoff Volcano samples. A: Pilot Pinnacle sample CALV053, D - dickite, I - illite, T - anatase. B: Pilot Pinnacle sample CALV069, K - kaolinite, J - jarosite, P - pyrophyllite, N - natroalunite. C: Little Hot Springs Valley Sample CALV 147, M - montmorillonite, I - illite, C - chlorite, O - orthoclase. D: Sulphur Works sample CALV196, K - kaolinite, A - alunite, Op - opal, T - anatase. E: Bumpass Hell sample CALV200, J - jarosite, A - alunite, Q - quartz, Op - opal, T - anatase, H - hematite. F: Bumpass Hell sample CALV201, A - alunite, C - cristobalite.

Figure 8. Scanning electron microscope images of hydrothermal alteration textures and minerals at Brokeoff Volcano. Black scale bars are at 10 mm. A: Bumpass Hell sample

CALV202 at 1000x magnification. Fine grained (<3-4 mm) alunite crystals growing on kaolinite. B: Sample CALV202 at 1500x magnification. C: Sample CALV104 from Little Hot Springs Valley at 500x magnification showing pyrite crystals in an illite/smectite groundmass. D: 3000x magnification of CALV104 showing illite/smectite crystals. E: Sample CALV147 from LittlHot Springs Vally at 1000x magnification showing montmorillonite crystals growing on coarse orthoclase. F: Sample CALV069 at 1000x magnification from Pilot Pinnacle. Jarosite crystals occur as fine grained crystals growing along the surface. Pyrophyllite occurs as coarse 5-10 mm platy crystals within cavities. G: Sample CALV097 from Little Hot Springs Valley at 1000x magnification showing coarse vuggy calcite crystalization. H: Sample CALV003 from Little Hot Springs Valley at 500x magnification showing chlorite/smectite alteration of mafics in the groundmass around feldspar grains.

Figure 9. Photographs of alteration and hydrothermal features. A: Western slopes of LHSV. Left section of photgraph shows alternating andesite lava flow and altered flow breccias. Lava flows have weak to no smectite alteration, breccias have pervasive montmorillonite, pyrite, illite/smectite, chlorite, albite, orthoclase, quartz, and calcite alteration. Pyrite is fine grained and forms small veins locally but not stockwork. To the right of the photo landslide and slump deposits have been completely altered to kaolinite/alunite/opal. Active steam vents are spread through out the area as well as the base of the valley. Smectite alteration also occurs with kaolinite suggesting possible overprint of younger steam heated alteration on the older near-neutral alteration. Rectangular insert denotes location of photo B. B: Upper section of LHSV with heavy set line marking contact where chlorite and calcite are distinctly missing in the upper sides of the slope. Alteration above line consists of montmorillonite, pyrite, illite/smectite, and silica. C: Photograph of Bumpass Hell looking to the northwest. Central part of the active vents and thermal pools is opal/kaolinite dominant with active sulphur mineralization. Altered slopes above the main active zone are alunite dominant.

Figure 10. Graph of δD versus $\delta^{18}O$ for water and steam samples from the Lassen region (data of Janik et al. [1983]). Lassen meteoric waters (solid triangles) define a line $\delta D = 8\ \delta^{18}O + 12$ reflecting regional storm direction. Acid sulfate waters (open circles) define an evaporation trend with a slope of ~3. Chloride waters of Morgan and Growler hot springs (solid circles) and superheated fumeroles from Bumpass Hell and Little Hot Springs Valley (solid squares) have similar δD meteoric water values, but have an $\delta^{18}O$ shift of +2 and +4 per mil.

Tables

1. Hydrothermal alteration assemblages at Brokeoff Volcano, California.
2. Deuterium values for clay, silt, and whole rock samples from Brokeoff Volcano, California
3. Geochemistry

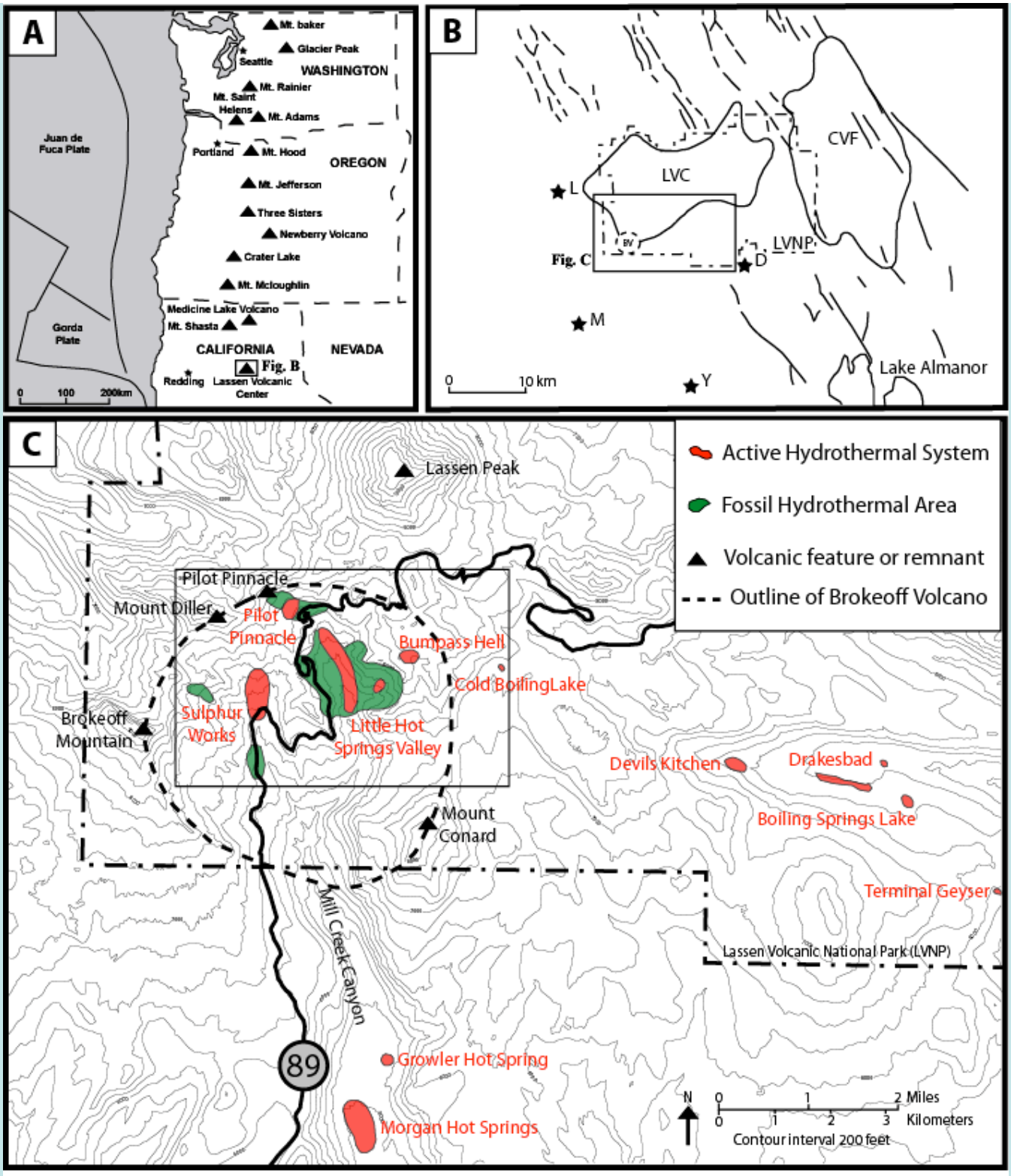

Figure 1. A: Tectonic setting of the Cascade Arc with rectangular insert denoting location of Lassen volcanic region. B: Map of the the Lassen volcanic region showing the major normal vaulting in the area. Irregular lines outline the vent fields of Lassen volcanic center (LVC) and Caribou volcanic field (CVF). Stars denote the locations of the other major volcanic centers: L, Latour; Y, Yana; D, Dittmar; and M, Maidu. Brokeoff volcano (BV) is dashed circle. Figure modified from Ingebritsen and Sorey (1985) and Guffanti et al. (1996). C: South east section of the Lassen region showing active hydrothermal systems in red and fossilized systems in green. Modified from Clynne et al. (2002). Solid rectangle marks location of figure 2.

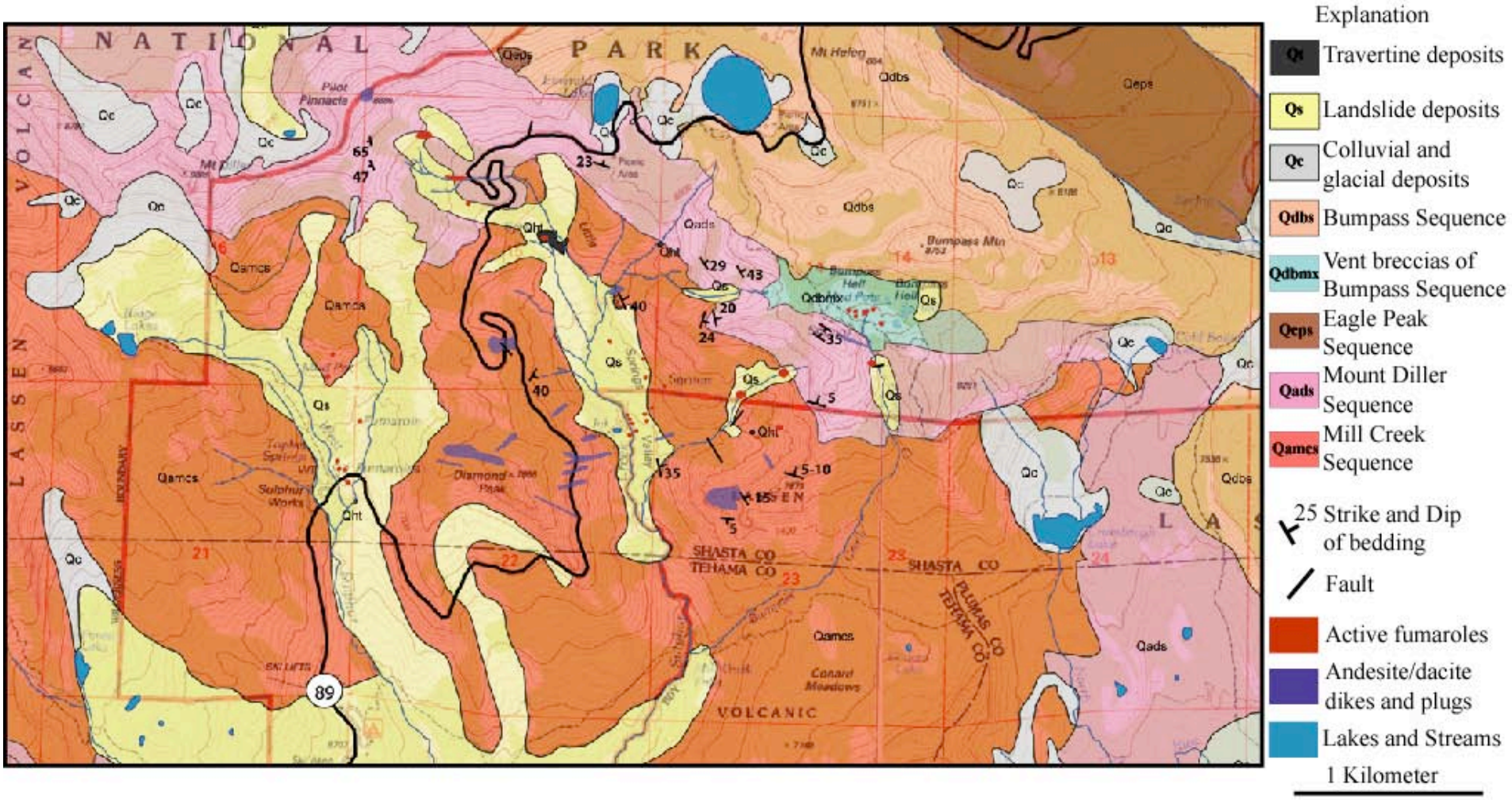

Figure 2. Geologic map of the Brokeoff Volcano region showing rock sequences, structure, active fumaroles and intrusive dikes and plugs. Geology from Clynne and Muffler (in press) and this study.

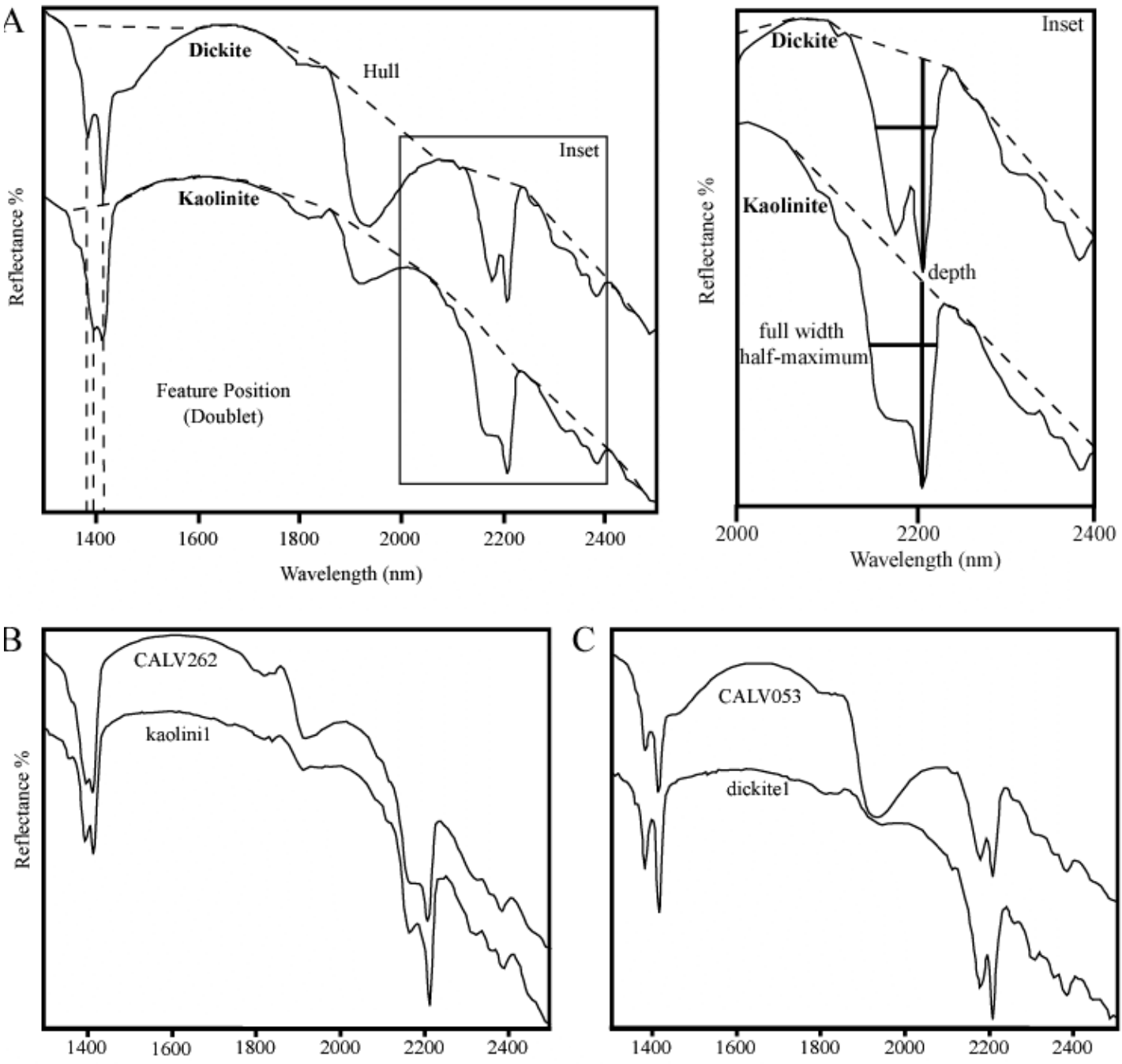

Figure 3. A: Infrared spectra of dickite and kaolinite (samples CALV053 and CALV262) showing the distinguishing characteristics for identification including the hull, feature depths, position, and the full width half-maximum. Dickite has doublet feature depths at 1.384 and 1.414, while kaolinite has doublet feature depths at 1.396 and 1.414. Kaolinite also has a higher full width half-maximum (inset). B: Spectra patterns of sample CALV262 vs. USGS Denver kaolinite standard. C: Spectra patterns of sample CALV053 vs. USGS Denver dickite standard. Large absorbance at 1.9 in CALV053 is from excess water in the sample as apposed to the standard.

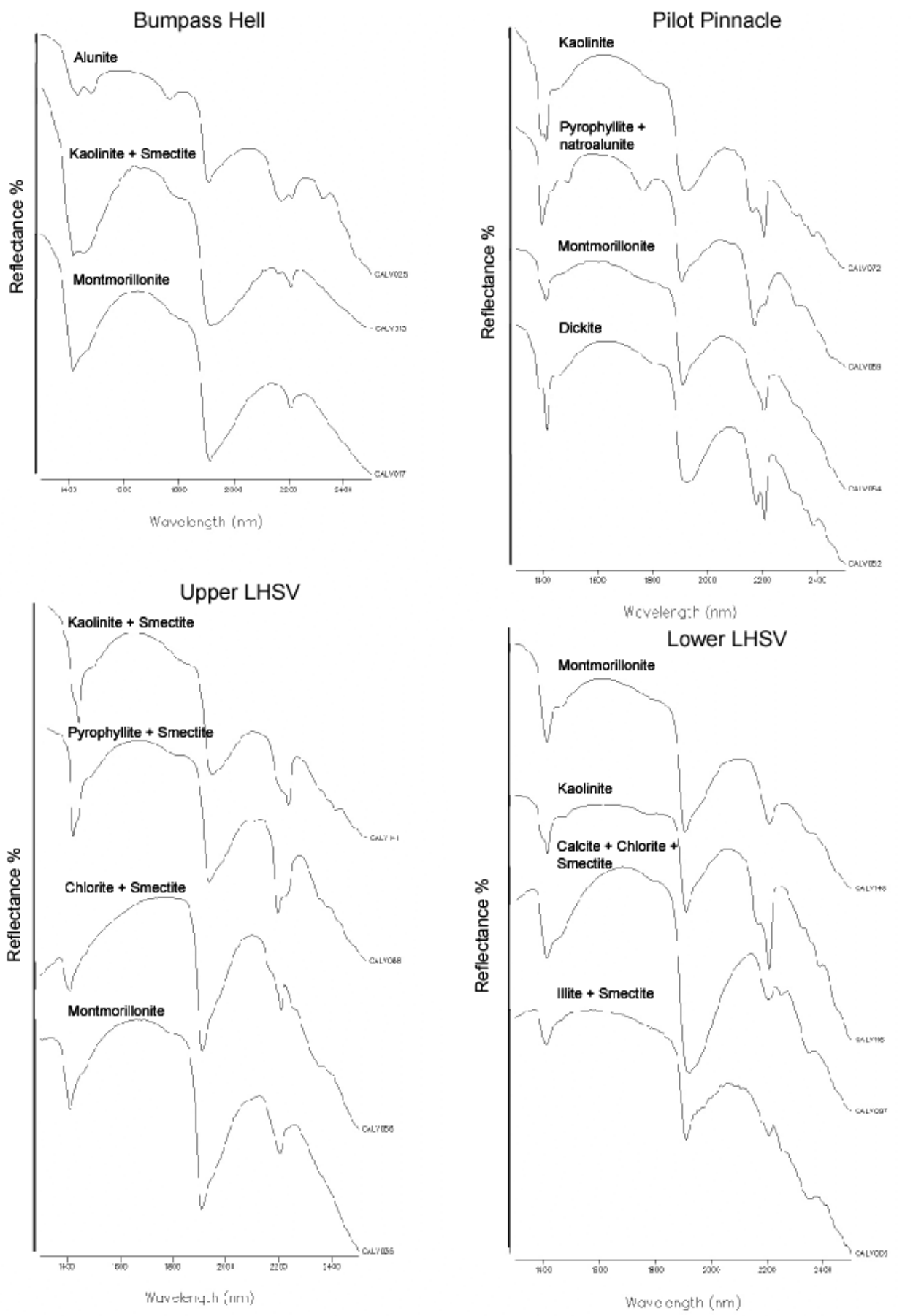

Figure 4. Infrared spectroscopy images from Bumpass Hell, Pilot Pinnacle, Upper Little Hot Springs Valley (LHSV), and Lower Little Hot Springs Valley (LHSV). Numbers to right of pattern indicate sample name and bold face mineral name/mixture above pattern indicates sample type.

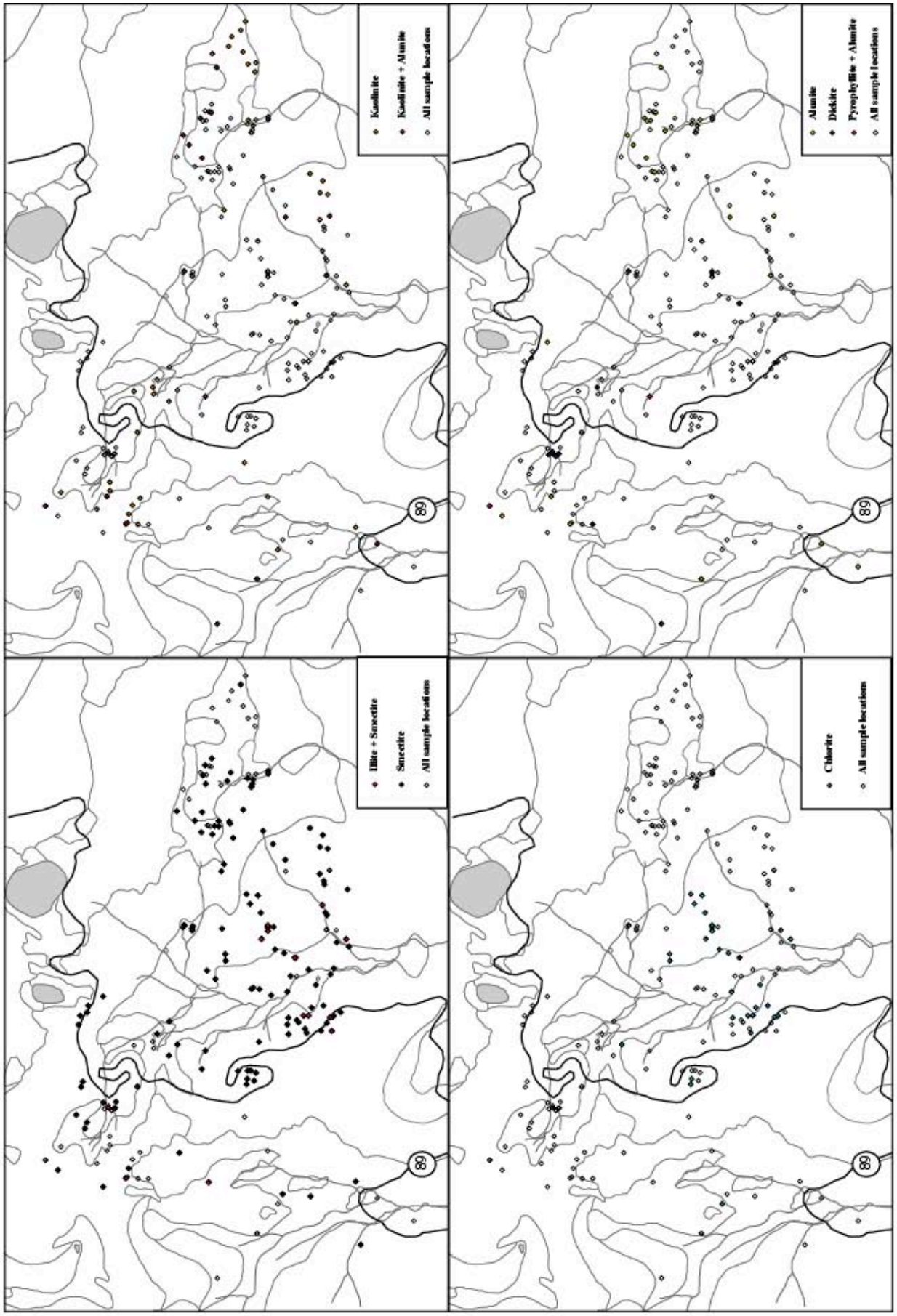

Figure 5. Sample maps denoting major mineral locations for the Brokeoff volcano area. Geology contacts same as in Figure 2.

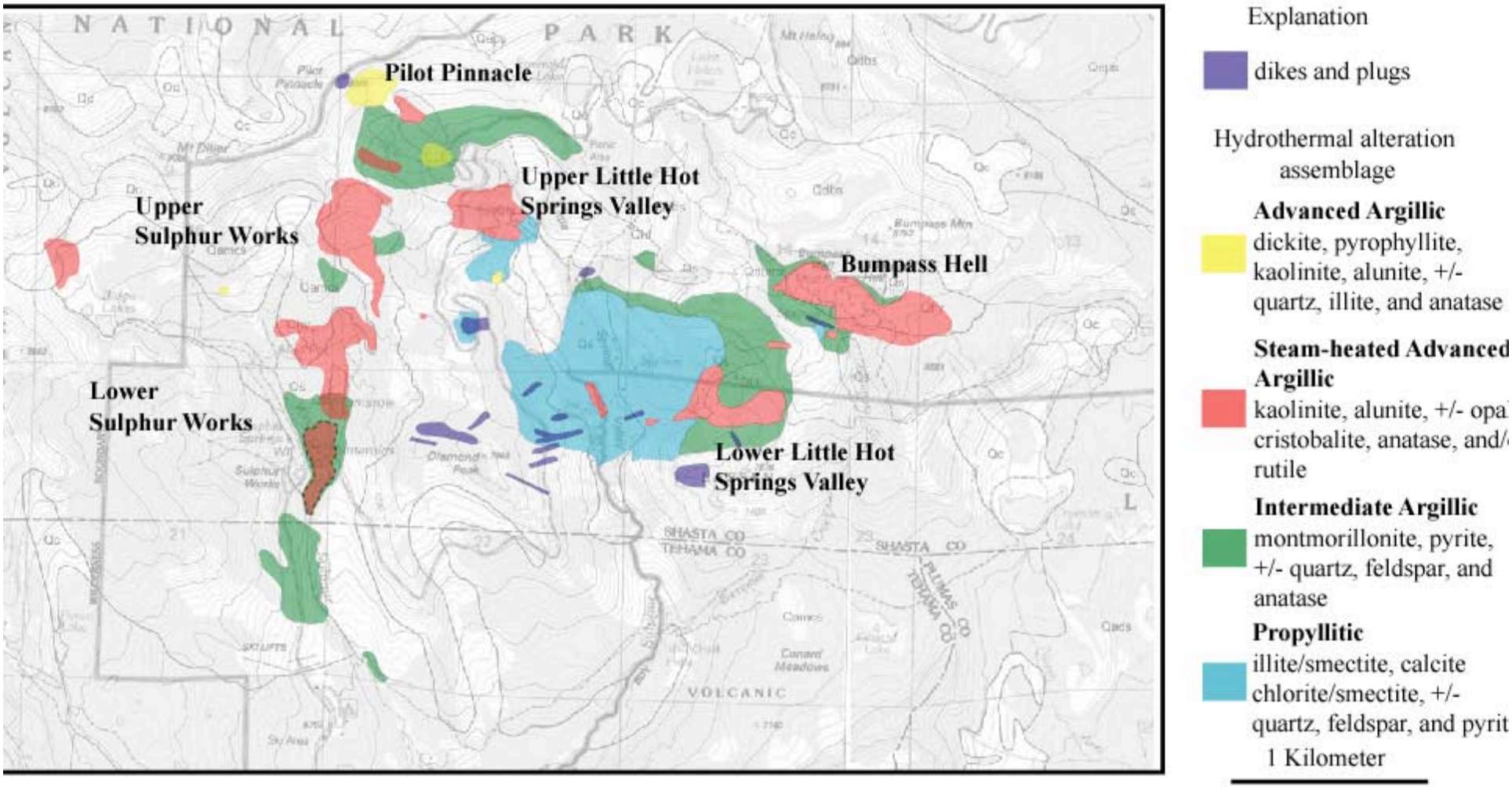

ıre 6. Map of the hydrothermal alteration assemblages in the Brokeoff Volcano region. Geologic contacts are same as in figure 2.

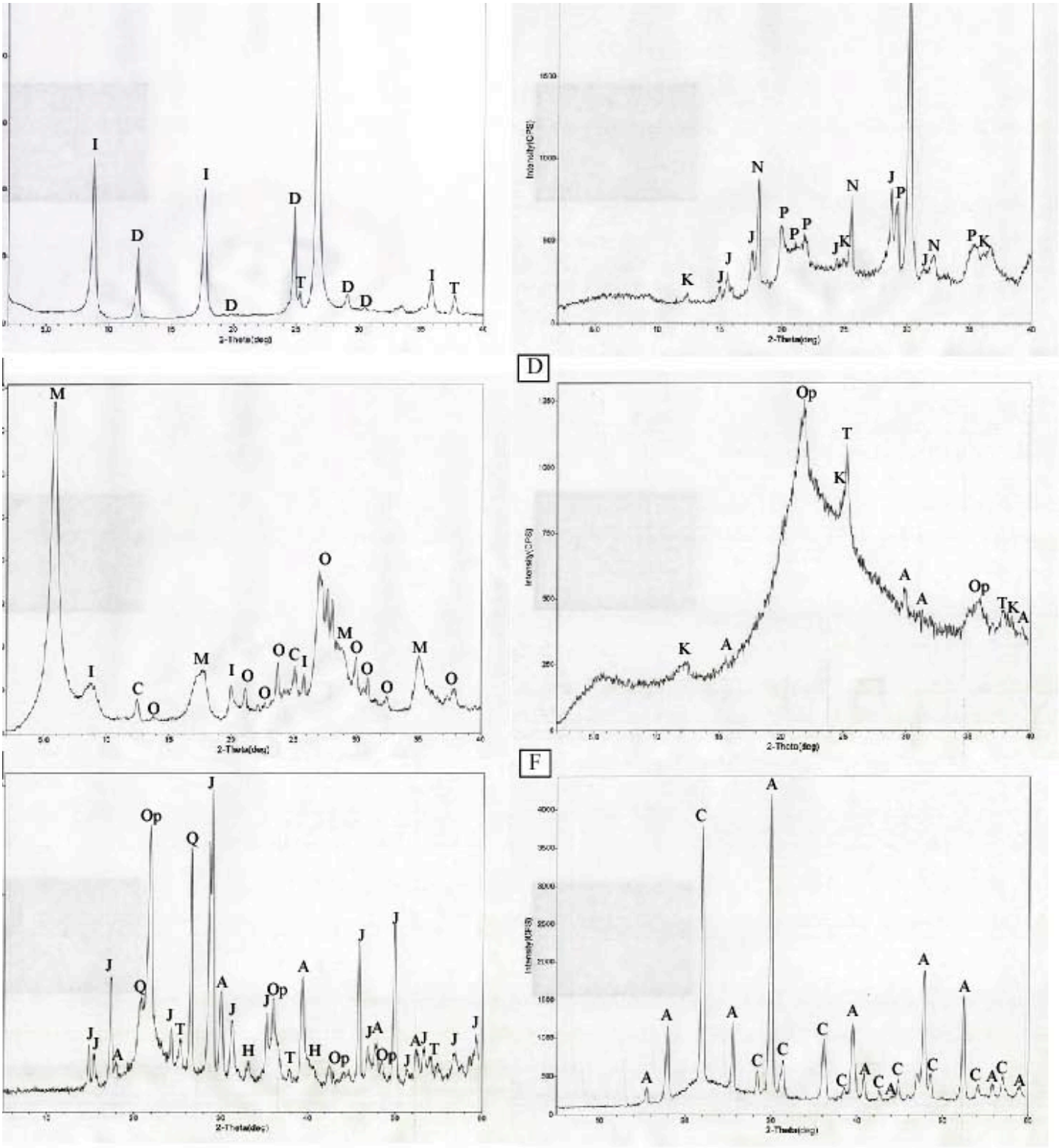

gure 7. XRD spectral patterns for Brokeoff Volcano samples. A: Pilot Pinnacle sample CALV053, D - dickite, I - ite, T - anatase. B: Pilot Pinnacle sample CALV069, K - kaolinite, J - jarosite, P - pyrophyllite, N - natroalunite. : Little Hot Springs Valley Sample CALV 147, M - montmorillonite, I - illite, C - chlorite, O - orthoclase. D: ılphur Works sample CALV196, K - kaolinite, A - alunite, Op - opal, T - anatase. E: Bumpass Hell sample ALV200, J - jarosite, A - alunite, Q - quartz, Op - opal, T - anatase, H - hematite. F: Bumpass Hell sample ALV201, A - alunite, C - cristobalite.

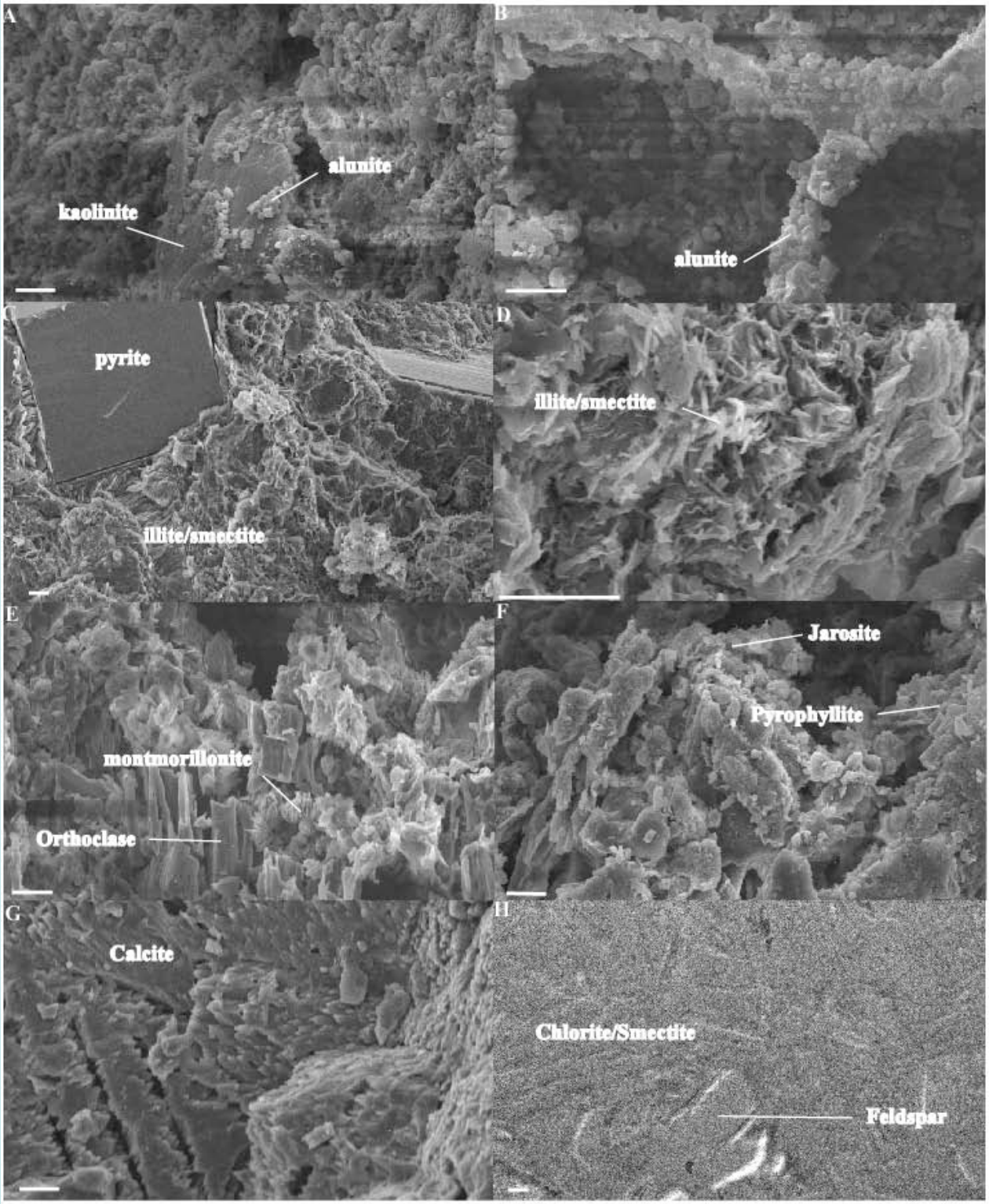

Figure 8. Scanning electron microscope images of hydrothermal alteration textures and minerals at Brokeoff Volcano. Black scale bars are at 10 µm. A: Bumpass Hell sample CALV202 at 1000x magnification. Fine grained (<3-4 µm) alunite crystals growing on kaolinite. B: Sample CALV202 at 1500x magnification. C: Sample CALV104 from Little Hot Springs Valley at 500x magnification showing pyrite crystals in an illite/smectite groundmass. D: 3000x magnification of CALV104 showing illite/smectite crystals. E: Sample CALV147 from LittlHot Springs Vally at 1000x magnification showing montmorillonite crystals growing on coarse orthoclase. F: Sample CALV069 at 1000x magnification from Pilot Pinnacle. Jarosite crystals occur as fine grained crystals growing along the surface. Pyrophyllite occurs as coarse 5-10 µm platy crystals within cavities. G: Sample CALV097 from Little Hot Springs Valley at 1000x magnification showing coarse vuggy calcite crystalization. H: Sample CALV003 from Little Hot Springs Valley at 500x magnification showing chlorite/smectite alteration of mafics in the groundmass around feldspar grains.

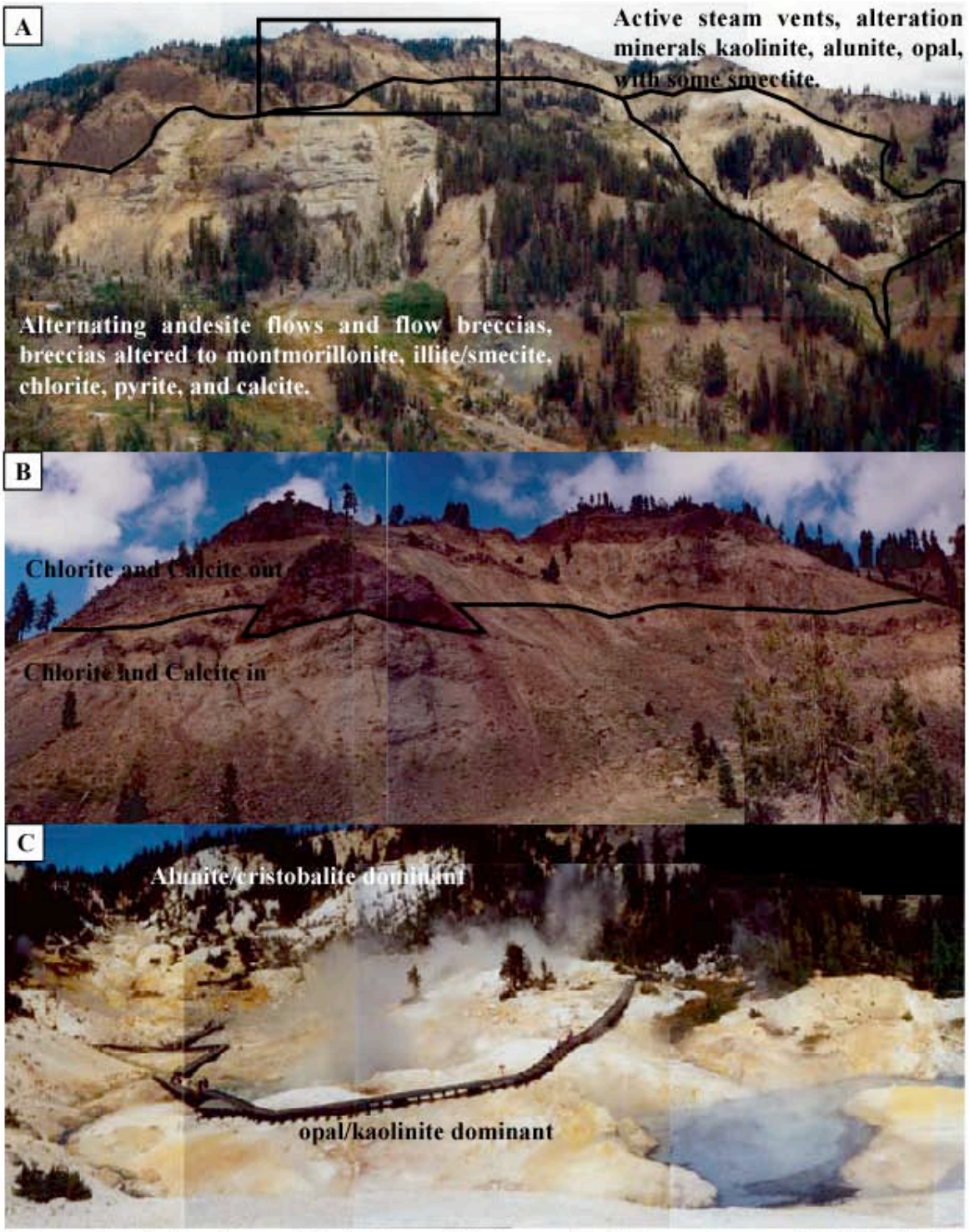

Figure 9. Photographs of alteration and hydrothermal features. A: Western slopes of LHSV. Left section of photgraph shows alternating andesite lava flow and altered flow breccias. Lava flows have weak to no smectite alteration, breccias have pervasive montmorillonite, pyrite, illite/smectite, chlorite, albite, orthoclase, quartz, and calcite alteration. Pyrite is fine grained and forms small veins locally but not stockwork. To the right of the photo landslide and slump deposits have been completely altered to kaolinite/alunite/opal. Active steam vents are spread through out the area as well as the base of the valley. Smectite alteration also occurs with kaolinite suggesting possible overprint of younger steam heated alteration on the older near-neutral alteration. Rectangular insert denotes location of photo B. B: Upper section of LHSV with heavy set line marking contact where chlorite and calcite are distinctly missing in the upper sides of the slope. Alteration above line consists of montmorillonite, pyrite, illite/smectite, and silica. C: Photograph of Bumpass Hell looking to the northwest. Central part of the active vents and thermal pools is opal/kaolinite dominant with active sulphur mineralization. Altered slopes above the main active zone are alunite dominant.

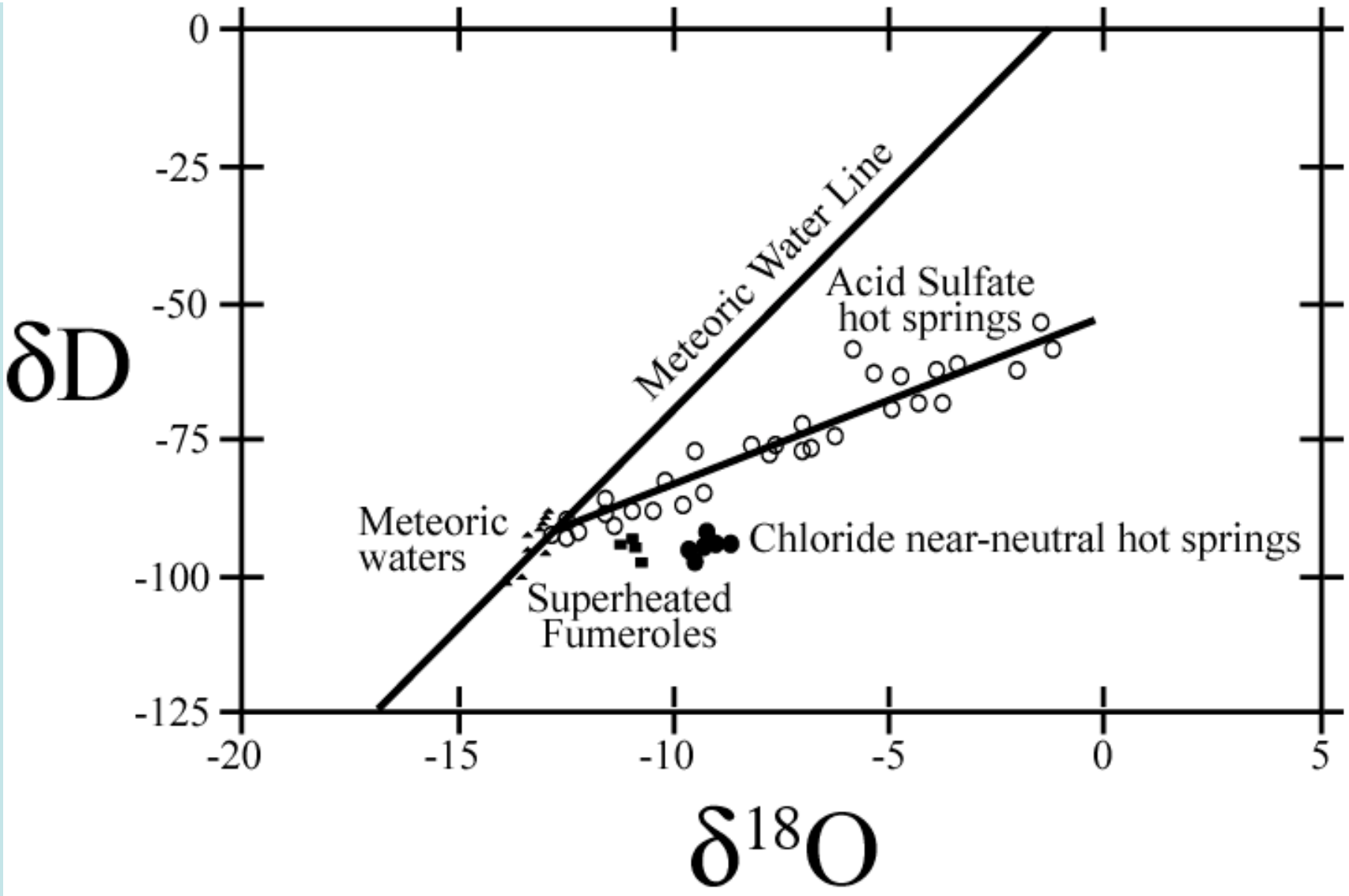

Figure 10. Graph of δD versus $\delta^{18}O$ for water and steam samples from the Lassen region (data of Janik et al. [1983]). Lassen meteoric waters (solid triangles) define a line $\delta D = 8\ \delta^{18}O + 12$ reflecting regional storm direction. Acid sulfate waters (open circles) define an evaporation trend with a slope of ~3. Chloride waters of Morgan and Growler hot springs (solid circles) and superheated fumeroles from Bumpass Hell and Little Hot Springs Valley (solid squares) have similar δD meteoric water values, but have an $\delta^{18}O$ shift of +2 and +4 per mil.

Table 1. Hydrothermal alteration assemblages at Brokeoff Volcano, California.

Assemblage[1]	Major Minerals	Accessory Minerals	Locations	Notes
SHAS	kaolinite, montmorillonite, alunite, natoralunite, opal, cristobalite	anatase, goethite, jarosite, hematite, Fe-sulfate minerals, native sulfur	Bumpass Hell, LHSV, Sulphur Works	Travertine deposits located in LHSV, and lower Sulphur Works in association with SHAS
AA	pyrophyllite, alunite, smectite, dickite, quartz	anatase, jarosite, goethite, illite	Pilot Pinnicle, Upper LHSV	
IA	montmorillonite, pyrite, illite, albite, quartz	anatase	Bumpass Hell, LHSV, Sulphur Works, Pilot Pinnacle	
PR	chlorite/smectite, calcite, montmorillonite, quartz,	anatase	LHSV,	

1. Assemblage names steam-heated acid sulfate (SHAS), advanced argillic (AA), intermediate argillic (IA), propylitic (PR).

Table 2. Hydrogen isotopic composistion of whole rock and <15 μm size fractions from Brokeoff Volcano, California

Sample Name	Location	Sample type	Geothermal System	Amount (mg)	PIMA	XRD
CALV013	Bumpass Hell	<15 μm	Active	0.983	Kaolinite/Smectite	Albite, Kaol-Mont, Mg-Smectite,
CALV017	Bumpass Hell	<15 μm	Active	1.120	Smectite	Albite, Montmorillonite, Cristobalite, Orthoclase
CALV025	Bumpass Hell	<15 μm	Active	1.700	Alunite	Cristobalite, Natroalunite
CALV069	Pilot Pinnacle	<15 μm	Inactive	1.310	Pyrophyllite/Na-alunite	Natroalunite, Jarosite, Kaolinite, Pyrophyllite
CALV075	Upper LHSV	<15 μm	Inactive	1.015	Kaolinite/Smectite	Kaolinite, Quartz, Mg-smectite
CALV086	Pilot Pinnacle	<15 μm	Inactive	1.940	Dickite	Dickite, Quartz, Anatase
CALV097	Lower LHSV	<15 μm	Inactive	2.130	Calcite/Chlorite/Smec	Mg-Fe Chlorite, Illite, Quartz, Albite, Hematite
CALV098	Lower LHSV	<15 μm	Inactive	1.860	Calcite/Chlorite/Smec	Mg-Fe Chlorite, Illite, Quartz, Albite, Hematite
CALV115	Lower LHSV	<15 μm	Active	1.580	Kaolinite	Kaolinite, Cristobalite, Quartz, Natroalunite
CALV121	Lower LHSV	<15 μm	Active	1.370	Alunite	Quartz, Kaolinite, Natroalunite, Jarosite, Goethite
CALV138	Lower LHSV	<15 μm	Active	1.210	N/A	Quartz, Albite, Illite, Montmorillonite, Anatase, Jarosite
CALV147	Lower LHSV	whole rock	Inactive	1.140	Smectite	Mont, Albite, Orthoclase, Mg-Fe Chlorite, Quartz, Illite
CALV148	Lower LHSV	whole rock	Inactive	1.108	Smectite	Montmorillonite, Orthoclase, Quartz, Illite
CALV149	Lower LHSV	whole rock	Inactive	1.671	Smectite	Quartz, Orthoclase, Mont, Illite, Mg-Fe Chlorite, Kaolinite
CALV153	Lower LHSV	<15 μm	Inactive	1.375	Chlorite/Smectite	Quartz, Albite, Mg-Fe Chlorite, Montmorillonite
CALV184	Sulphur Works	<15 μm	Inactive	1.340	N/A	Natroalunite, Quartz, Cristobalite, Kaolinite

Table 3

Sample	CALV006	CALV015	CALV025	CALV052	CALV053	CALV069	CALV072	CALV077	CALV088	CALV097	CALV111	CALV138	CALV147	CALV148	CALV149	CALV175	CALV178	CALV184	CALV187	CALV195	CALV198	CALV202	CALV204	CALV207
Alteration	PR	SHAS	SHAS	AA	AA	AA	SHAS	SHAS	AA	PR	PR	IA	PR	IA	PR	SHAS	SHAS	SHAS	SHAS	SHAS	SHAS	SHAS	SHAS	IA
Wt. %																								
Al	7.8	0.57	2.59	0.96	13.2	6.76	9.37	8.35	9.99	3.4	10.58	6.67	8.03	5.56	6.8	8.72	8.6	9.73	9.66	6.37	0.31	8.92	2.2	4.61
Ca	3.17	0.01	0.08	0.11	0.01	0.3	0.08	0.16	0.17	20.9	1.79	1.51	0.18	0.07	0.04	0.28	0.21	0.09	0.02	0.28	0.13	1.13	0.12	0.85
Fe	3.66	0.39	0.62	0.07	0.05	9.34	0.09	0.22	1.77	1.89	4.82	2.46	1.07	0.64	0.21	0.57	0.3	2.41	0.4	2.81	0.03	1.53	0.34	0.72
K	1.63	0.17	0.74	0.07	0.38	0.87	0.1	0.53	2.18	0.64	0.87	2.01	3.48	3.59	2.27	1.94	1	1.8	2.16	1.31	0.03	1.46	1.07	0.15
Mg	1.99	<0.01	0.02	0.02	0.03	0.13	0.03	0.19	0.15	0.78	1.87	0.79	0.41	0.27	0.37	0.25	0.11	0.09	0.12	0.41	0.02	0.83	0.02	0.33
Na	1.72	0.02	0.31	0.02	0.02	0.81	0.05	0.51	0.33	0.75	2.15	1.36	0.56	0.11	0.08	0.64	0.19	0.5	0.3	0.59	0.01	1.65	0.14	0.78
S	0.52	0.44	1.41	0.24	0.03	3.46	0.34	0.34	0.2	0.93	0.02	0.78	0.17	0.02	0.07	4.39	0.94	4.63	0.3	0.09	0.03	0.22	0.09	0.1
Ti	0.36	0.44	0.47	0.54	0.59	0.28	0.46	0.53	0.51	0.17	0.58	0.37	0.31	0.48	0.32	0.41	0.51	0.39	0.14	0.51	0.35	0.34	0.41	0.24
ppm																								
Au	<0.005	<0.005	<0.005	<0.005	<0.005	<0.005	<0.005	0.006	<0.005	<0.005	<0.005	0.009	<0.005	<0.005	<0.005	<0.005	<0.005	<0.005	<0.005	<0.005	<0.005	<0.005	<0.005	<0.005
Hg	0.04	1.54	1.4	0.23	0.04	0.37	0.25	1.58	<0.02	<0.02	0.23	0.1	0.24	0.06	1.08	0.14	1.46	1.99	0.09	4.4	2.96	0.08	2.18	1.36
Ag	<1	<1	<1	<1	<1	<1	<1	<1	<1	<1	<1	<1	<1	<1	<1	<1	<1	<1	<1	<1	<1	<1	<1	<1
As	6	6	4	18	10	19	10	53	111	5	3	4	4	10	5	5	14	11	11	4	3	4	6	9
Ba	495	489	606	740	599	669	453	537	907	243	390	755	1160	1700	471	393	575	422	768	499	207	599	676	436
Be	1	<0.1	0.4	0.2	0.1	1.4	0.4	0.8	0.6	0.5	1.1	1	0.8	0.6	1	0.4	0.7	0.3	0.5	0.6	0.4	1.1	0.8	0.5
Bi	0.1	0.06	0.14	10.3	0.59	0.09	0.11	0.13	0.2	0.05	0.07	0.12	<0.04	<0.04	<0.04	0.08	0.26	0.08	1.3	<0.04	0.06	0.08	0.08	0.05
Cd	<0.1	<0.1	<0.1	<0.1	<0.1	<0.1	<0.1	<0.1	<0.1	<0.1	<0.1	<0.1	<0.1	<0.1	<0.1	<0.1	<0.1	<0.1	<0.1	<0.1	<0.1	<0.1	<0.1	<0.1
Ce	30.1	30.2	20.3	65.9	21.2	35.5	42.5	50.9	38.1	18	45.6	29.3	38.6	39.5	48.2	21.7	35.5	195.9	10.2	11.7	0.33	28.4	17.3	24.6
Co	17.6	0.3	0.3	0.4	<0.1	0.9	<0.1	0.2	0.4	8	20.5	11.3	0.2	0.2	0.2	2.8	1.4	1	1.1	2.2	<0.1	6.7	0.3	4.1
Cr	21	10	23	24	55	43	53	55	68	17	31	22	4	3	3	196	24	42	31	28	4	26	3	27
Cs	0.72	0.2	1.17	<0.05	<0.05	1.79	1.17	1.52	0.36	0.29	1.01	0.8	1.5	0.97	1.68	0.56	2.11	0.4	0.75	0.62	0.07	1.07	3.09	0.69
Cu	47.6	2.4	6.6	4.3	9.8	30.1	5	2.6	9.5	21	74.8	48.8	2.8	9.6	3.9	26	11.3	50.8	23.6	18	3.9	25.8	9	11.9
Ga	13.9	9.24	13.5	2.63	19.4	12.9	12.5	12.8	14.9	6.07	18.5	14	19	12.4	13.2	22.7	14.2	15.9	12.1	14.2	0.34	16.1	4.12	9.02
In	0.05	<0.02	0.02	<0.02	<0.02	0.02	<0.02	0.04	0.03	<0.02	0.06	0.04	0.03	0.03	<0.02	0.04	<0.02	0.05	0.03	0.03	<0.02	0.04	<0.02	0.02
La	13.6	15.8	10.1	30.5	9.8	15.8	19.6	21.1	16.9	8.9	21	15.6	19.3	20.5	23.1	9.3	15.5	78.9	4.5	6.1	<0.5	13.2	7.9	11.7
Li	13	<1	<1	2	18	8	73	13	16	3	13	10	3	3	6	15	58	1	4	3	<1	7	1	3
Mn	639	13	24	13	<5	52	6	69	38	866	842	258	30	31	61	25	35	36	18	206	18	255	42	57
Mo	0.12	0.85	1.22	2.77	2.48	1.44	1.61	1.22	1.41	0.18	0.56	0.21	0.08	1.95	0.5	0.56	1.53	1.3	1.25	1.52	1.13	0.91	2.18	0.93
Nb	5.3	7.2	7.5	8.7	7.9	5.5	8.2	8.4	6	2.5	8.6	5.4	8.4	11.3	6.8	3.3	5.7	6.1	2.5	4.5	3.9	6	7.7	4.5
Ni	42.2	1.2	1	0.7	0.8	4.6	1.9	1.5	2.7	16.3	39.6	21.1	1.1	0.9	0.7	6.6	3.6	3.5	4.7	7.2	<0.5	21.1	1	10.8
P	705	330	492	1240	143	2920	1020	2010	2020	383	1180	589	296	<50	138	836	1070	2420	1210	291	<50	407	72	173
Pb	8.9	10.1	11.6	14	4.8	10.3	9.6	16.4	9.5	4	6.6	9.2	26.8	9.3	13	8.8	7.6	15.1	13	7.1	1.9	9.8	9.7	5.7
Rb	55.4	3	27.6	1.8	12.3	21.7	7.4	20.1	40.5	17.7	26.6	58.7	130.3	127.2	95.5	12.9	40.7	29.6	45.4	43.7	1.8	40.8	56	5.3
Sb	0.38	0.3	0.83	2.82	2.04	0.81	0.74	1.32	8.39	0.17	0.22	0.4	0.59	0.92	0.73	0.38	0.63	0.43	1.39	0.26	0.16	0.43	0.65	0.38
Sc	13.5	5.6	4	3.9	5.5	10.4	8.8	8.1	6.6	6.8	19.9	12.5	8.2	11	7	20.1	19.3	22.9	9.6	11.6	0.7	10.9	1.9	6.3
Sn	0.9	1.1	1.3	2.2	1.5	1.1	1.2	1.1	1.1	0.4	1.2	1.3	1.1	1.4	1	1.1	0.9	1	1.4	1.2	0.7	1	1.3	0.7
Sr	353.1	166.9	313.1	736.7	44.3	1331.3	968.6	1215.2	613.8	458.3	382.2	444.4	83.3	61.4	30.7	783.9	557.5	1142.8	341.1	103.3	37.9	305.2	36.5	175.8
Te	<0.1	<0.1	<0.1	0.5	0.3	1.1	<0.1	0.9	1.1	<0.1	<0.1	<0.1	<0.1	<0.1	<0.1	0.5	<0.1	<0.1	0.2	<0.1	<0.1	<0.1	<0.1	<0.1
Th	4.2	9.3	6.1	8.6	2.6	6	6.4	5.4	5.4	1.8	6.4	3.7	8.9	11.7	8.3	2.2	5	6.8	1.4	5	0.2	6.6	6.5	1.3
Tl	0.2	<0.1	0.1	<0.1	0.3	0.5	<0.1	0.5	0.3	<0.1	0.1	0.3	0.5	0.3	0.3	0.2	0.4	0.1	1.3	0.2	<0.1	0.3	0.3	0.2
U	1.4	3.3	1.4	1.3	0.5	1.9	1.3	1	0.8	0.6	2.1	1.2	1.4	4.6	2.6	0.4	1.8	2.7	0.2	1.7	0.3	2.6	2.5	0.8
V	124	30	36	47	188	147	132	134	190	60	166	121	57	46	44	231	191	204	135	123	8	91	13	56
W	0.3	0.6	0.7	0.6	0.8	0.7	0.9	0.5	0.8	0.2	0.8	0.4	0.4	1.1	0.7	0.4	0.7	0.5	0.4	0.5	0.1	0.5	1	0.3
Y	13	7.5	3.6	4.1	1.7	7.3	5.7	3.9	4.1	8.2	20.4	8.9	12	12.4	10.5	1.5	5	9.8	1.4	5.6	0.2	12.2	7.1	8.6
Zn	52	2	4	5	9	21	7	33	28	24	91	30	7	6	7	13	9	11	6	17	2	29	8	16